SCIENTIFIC REPORTS

OPEN

SUBJECT AREAS:
OPTICAL MATERIALS AND STRUCTURES
MATERIALS FOR OPTICS

Received
28 October 2013

Accepted
9 December 2013

Published
9 January 2014

Correspondence and requests for materials should be addressed to D.P.C. (dpchen2008@aliyun.com)

2.7 μm emission of high thermally and chemically durable glasses based on AlF_3

Feifei Huang[1,2], Yaoyao Ma[1,2], Weiwei Li[1,2], Xueqiang Liu[1,2], Lili Hu[1] & Danping Chen[1]

[1]Key Laboratory of Materials for High Power Laser, Shanghai Institute of Optics and Fine Mechanics, Chinese Academy of Sciences, Shanghai 201800, PR China, [2]Graduate School of Chinese Academy of Sciences, Beijing 100039, PR China.

AlF_3-based glasses (AlF_3-YF_3-CaF_2-BaF_2-SrF_2-MgF_2) with enhanced thermal and chemical stability were synthesized and compared with the well-known fluorozirconate glass (ZBLAN). The 2.7 μm mid-infrared emission in the AlF_3-based glasses was also investigated through the absorption and emission spectra. Both the temperature of glass transition and the characteristic temperatures (ΔT, H_r, k_{gl}) of the fluoroaluminate glasses were much larger than those of the ZBLAN glasses. The corrosion phenomenon can be observed by naked-eye, and the transmittance dropped dramatically (0% at 3 μm) when the ZBLAN glass was placed into distilled water. However, the AlF_3-based glass was relatively stable. The fluoroaluminate glasses possessed large branching ratio (20%) along with the emission cross section (9.4×10^{-21} cm^{-2}) of the Er^{3+}:$^4I_{11/2}\rightarrow{}^4I_{13/2}$ transition. Meanwhile, the enhanced 2.7 μm emission in highly Er^{3+}-doped AYF glass was obtained. Therefore, these results showed that this kind of fluoride glass has a promising application for solid state lasers at 3 μm.

Middle infrared fiber lasers at 3 μm region have potential application in eye-safe laser radar, monitoring atmospheric pollutants, and high-resolution spectroscopy of low-pressure gases[1–3]. In the recent years, the use of erbium-doped bulk solid state lasers for high-quality cutting or ablation of biological tissue caused by the high absorption of 3 μm radiation in water has been demonstrated[4,5]. The well-known 2.7 μm emission of Er^{3+} due to the $^4I_{11/2}\rightarrow{}^4I_{13/2}$ transition can be obtained pumped at 800 nm or 980 nm[6], and the lack of commercial high-power pump diodes that emit at 1100 nm or 1300 nm limits the application of holmium and dysprosium doped materials.

Fluoride glasses are potential candidates for IR optical fibers because of their middle infrared region transparency and low theoretical loss <0.01 dB/Km in the wavelength range of 2 μm to 5 μm, which is 10 times less than the silica fibers[7]. Most investigations focused on the fluoride glass host at the pioneer time and up to now only fluoride glass fiber lasers have been reported in the region of 3 μm. Over the past decades, the 10-W-level diode pumped 2.7 μm Er-doped ZBLAN fiber lasers was obtained[8–10]. However, the poor chemical durability, low mechanical strength, along with the low glass transition temperature (T_g), have limited the application of ZBLAN glass and scaling up the output power further is fundamentally difficult[11]. Thus, exploring effective host matrix becomes a challenge to the researchers. Oxide glass is one candidate with easy preparation, good physical and mechanical performance and good chemical durability. There has been attempt pouring into tellurite glass[12,13], bismuthate glass[14] and germinate glass[15] at present. On the other hand, new high thermally and chemically durable fluoride glasses should be considered and investigated based on the significant advantages of high solubility for rear earth ions, low maximum phonon energy as well as high mid-infrared transparency. By contrast, AlF_3-based glasses appear to be less susceptible to those problems that limit the further application of fluorozironate glasses[7,16]. H.Yanagita has reported the laser performances of Er^{3+}-doped fluorozircoaluminate[17]. However, no investigation has focused on the 2.7 μm emission properties of Er^{3+}-doped fluoroaluminate glasses so far.

The present work aims to investigate the various compositions of high thermally and chemically durable AlF_3-based glasses and compares their thermal and mechanical properties with the well-known ZBLAN glass. In addition, 2.7 μm emission of Er^{3+} in these AlF_3-based fluoride glasses is investigated for future application in mid infrared lasers, Judd-Ofelt intensity parameters, spontaneous transition probability and stimulated emission cross section were also calculated and discussed.

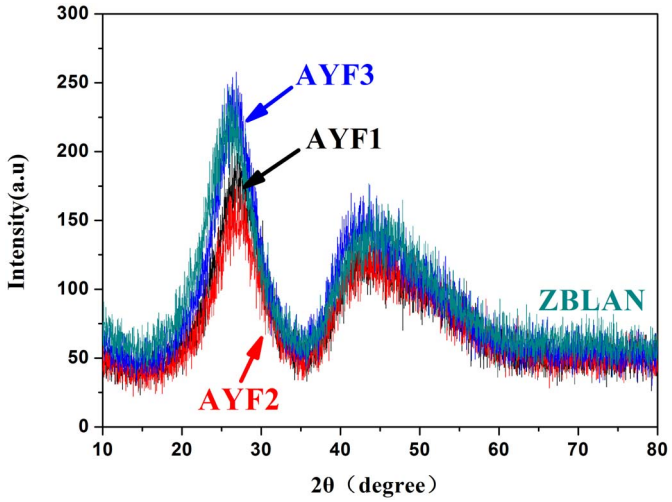

Figure 1 | XRD spectra of the present samples.

The investigated glasses have the following molar compositions: $35AlF_3$-$15YF_3$-$20CaF_2$-$10BaF_2$-$10SrF_2$-$10MgF_2$-$1ErF_3$ (AYF1), $40AlF_3$-$15YF_3$-$15CaF_2$-$10BaF_2$-$10SrF_2$-$10MgF_2$-$1ErF_3$ (AYF2), $37AlF_3$-$15YF_3$-$15CaF_2$-$13BaF_2$-$10SrF_2$-$10MgF_2$-$1ErF_3$ (AYF3), $37AlF_3$-$15YF_3$-$15CaF_2$-$13BaF_2$-$10SrF_2$-$10MgF_2$-$2ErF_3$ (AYF3-2), $37AlF_3$-$15YF_3$-$15CaF_2$-$13BaF_2$-$10SrF_2$-$10MgF_2$-$4ErF_3$ (AYF3-4), and $53ZrF_4$-$20BaF_2$-$4LaF_3$-$3AlF_3$-$20NaF$-$1ErF_3$ (ZBLAN).

The samples were prepared using high-purity AlF_3, YF_3, CaF_2, BaF_2, SrF_2, MgF_2, ZrF_4, LaF_3, NaF and ErF_3 powder. Well-mixed 25 g batches of the samples were placed in platinum crucibles and melted at about 1000°C for 30 min. Then the melts were poured onto a preheated copper mold and annealed in a furnace around the glass transition temperature. The annealed samples were fabricated and polished to the size of 20 mm×15 mm×1 mm for the optical property measurements.

The characteristic temperatures (temperature of glass transition T_g and temperature of onset crystallization peak T_x) of samples were determined using a NetzschSTA449/C differential scanning calorimetry at a heating rate of 10 K/min. Phases of the samples were characterized by X-ray diffraction (XRD, Rigaku RINT-2000) with Cu Kα radiation. The density and refractive indices of the samples were measured by the Archimedes method using distilled water as an immersion liquid and the prism minimum deviation method respectively. The concentration of the cationic species in water was measured by Inductively Coupled Plasma (ICP). Furthermore, the absorption spectra were recorded with a Perkin-Elmer Lambda 900 UV/VIS/NIR spectrophotometer in the range of 100 nm–1900 nm, and the emission spectra were measured with a Triax 320 type spectrometer (Jobin-Yvon Co., France). All the measurements were carried out at room temperature.

The transparent and homogeneous samples with the different compositions mentioned before have been obtained. Figure 1 shows the XRD (X-ray diffraction) spectra of the samples, all the samples have two dispersion peaks at approximately 25° and 47° which are the characteristic peaks of the fluoride glasses[18]. It is demonstrated that the prepared AlF_3-based fluoride glasses have good glass-forming ability and have not shown devitrification tendencies when being formed.

Table 1 | Characteristic temperatures (T_g, T_x, T_p, T_m) and ΔT, H_r, k_{gl} of present glasses

Glass	T_g(°C)	T_x(°C)	T_p(°C)	T_m(°C)	ΔT(°C)	H_r	k_{gl}
AYF1	428	509	529	900	81	0.218	0.171
AYF2	427	512	535	900	85	0.232	0.179
AYF3	438	520	539	900	82	0.227	0.177
ZBLAN	269	336	358	850	67	0.135	0.115

Table 1 presents the DSC results for AYF1, AYF2, AYF3 and ZBLAN glasses in this study. The glass criterion, $\Delta T = T_x - T_g$ (temperature of glass transition T_g, temperature of onset of crystallization T_x) was introduced by Dietzel[19,20] and is often regarded as an important parameter for evaluating the glass forming ability. ΔT has been frequently used as a rough criterion to measure glass thermal stability; a large ΔT means strong inhibition of nucleation and crystallization. Hruby[21] developed the H_r criterion, $H_r = \Delta T/(T_m - T_p)$, which includes the characteristic temperatures, where T_m is the melting temperature of the glass and T_p is the temperature of peak of crystallization. The glass formation factor of the materials is given by the parameter $k_{gl} = (T_x - T_g)/(T_m - T_g)$[20]. Compared with ΔT, it is more suitable to estimate the glass thermal stability. The larger the k_{gl}, the better forming ability the glass will have. The glass forming ability can be estimated by the given characteristic temperatures. The values of these characteristic temperatures among these three AlF_3-based glasses changed slightly. When AlF_3 was replaced by CaF_2 or MgF_2 partly, the values decreased slightly in some degree. However, the thermal stability of these AlF_3-based glasses is better than that of the ZBLAN sample. In addition, T_g is also an important factor for laser glasses, a high one such as 420+°C of the AlF_3-based glasses compared with other various fluorozirconate glasses (270°C–350°C)[22,23] provides good thermal stability to resist thermal damage at high pumping intensities.

The chemical durability of the sample was measured as follows: (3.1 shows that the three AlF_3-based glasses have similar thermal stability. The results of AYF2 and ZBLAN glasses are listed because they have the same regular pattern.). First, the weighted sample (W_1) was placed into the distilled water. Second, the sample was kept in a thermostatic water bath at 98°C for 5 h and then the samples were cooled and dried in a dying box at 70°C for 1 h. Finally, the dry sample was weighed again (W_2). The chemical durability of AYF2 and ZBLAN glasses was evaluated by the values of $\Delta W\% = \frac{w_1 - w_2}{w_1} \times 100\%$[24] and $\Delta W'\% = \frac{w_1 - w_2}{v_1} \times 100\%$. The ΔW%(111.5 mg/g)and ΔW'% (488.6 mg/cm³) of ZBLAN were 30 times larger than those of the AYF2 sample which were 3.3 mg/g and12.6 mg/cm³, respectively.

The surface layer of the ZBLAN corroded and became white after placing into distilled water for 24 hours at room temperature and the corrosion layer tended to peel off. The layer in contact with the water remained the same by naked-eye observation in the case of AlF_3-based glass. The cationic species Zr, Ba, La, Al, and Na (ZBLAN) and Al, Ba, Ca, Y, Sr, and Mg (AYF2) were measured through ICP (Inductively Coupled Plasma) and the results are shown in Table 2.

Table 2 | Concentration of cationic ions of based glass in water

Sample	Concentration of cationic in water					
ZBLAN (μg/ml)	Zr	Ba	Al	Na	La	
	0.1	0.23	0.09	127.0	-----	
AYF2 (μg/ml)	Al	Ba	Ca	Y	Sr	Mg
	0.25	0.17	3.0	--	0.35	1.0

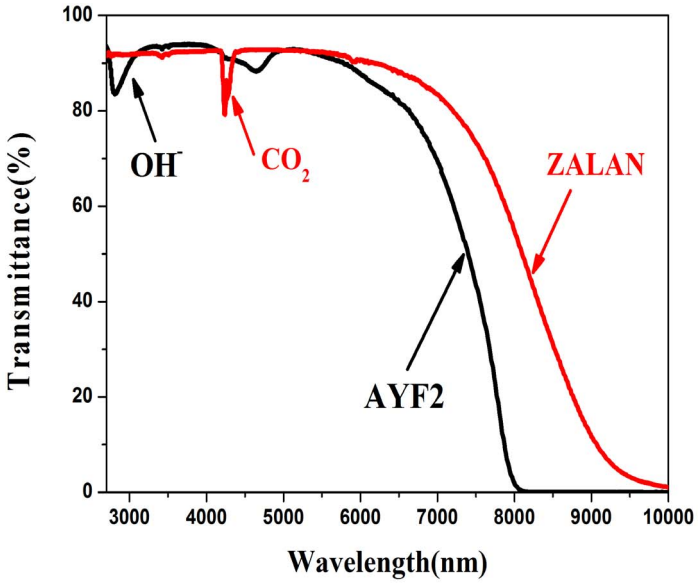

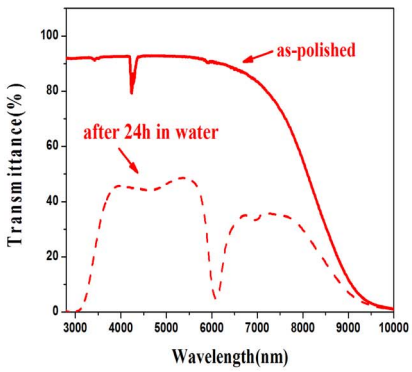

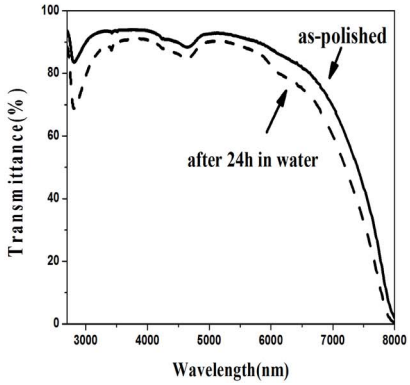

Figure 2 | (a): Transmittance spectra of the 1.0 mm thick AYF2 and ZBLAN samples. (b): The IR transmission spectra of ZBLAN glass before and after water treatment. (c): The IR transmission spectra of AYF2 glass before and after water treatment.

The concentration of the cationic of ZBLAN in water was much larger than that of AYF2. Therefore, NaF,AlF_3,CaF_2, MgF_2, SrF_2 and BaF_2 dissolve at faster rates than ZrF_4, LaF_3, and YF_3, as was also reported by T. Iqbal et al[7]. These results prove that the chemical stability of AYF2 is much better than that of ZBLAN glass.

Figure 2(a) shows the transmittance spectra of the 1.0 mm thick AYF2 and ZBLAN samples. The IR cut-off wavelength for ZBLAN is ~7 μm. The cut-off occurs instead at ~6 μm when Zr is largely replaced by light Al atoms in the AYF glass matrix, beacuse the Al-F fundamental vibrations shifted toward slightly high frequencies. The transmittance of AYF and ZBLAN samples reached as high as 93% and 90%, respectively. The ~10% loss contained the Fresnel reflections dispersion, and absorption of the glass. An OH^- absorption peak (~2.9 μm) exists in AYF2 sample, but the transmittance still reached above 83% at 2.9 μm. More study should be carried out further to deduce the concentration of the OH^- in the fluoroaluminate glasses in the future. Figures 2 (b) and (c) exhibits the IR transmission spectra of AYF2 and ZBLAN glasses before and after the water treatment, respectively. Change in the absorption band at 2.9 μm was because of the fundamental OH^- absorption. The transmittance of the ZBLAN sample dropped dramatically and was even completely light-tight in the region of 3 μm. The absorption around 6.2 μm because of the fundamental of fluoride glass also became

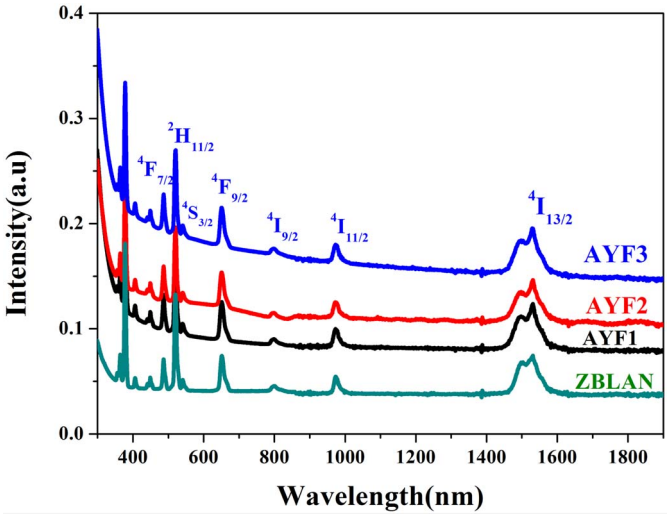

Figure 3 | **Absorption spectra of the samples at room temperature in the wavelength region of 300 nm–1900 nm.**

Table 3 | J-O parameters Ω_t of Er^{3+} in various glasses

	AYF1	AYF2	AYF3	ZBLAN	ZBLAY	ZBLN	phosphate
$\Omega_2(\times10^{-20}\ cm^{-2})$	1.59	1.36	1.56	2.70	3.08	2.60	6.65
$\Omega_4(\times10^{-20}\ cm^{-2})$	1.13	1.03	1.10	1.68	1.46	1.31	1.52
$\Omega_6(\times10^{-20}\ cm^{-2})$	1.01	0.95	1.05	1.18	1.69	1.12	1.11
$\delta(\times10^{-6})$	0.12	0.03	0.10	0.11	---	---	---
		This work			23	17	34

Table 4 | Calculated predicted spontaneous transition probability (A), radiaive lifetime (τ_{rad}), and branching ratio (β) of certain optical transitions for Er^{3+} - doped present glasses

	AYF1			AYF2			AYF3			ZBLAN		
Transition	A/S^{-1}	β/%	τ/ms	A	β	τ	A	β	τ	A	β	τ
$^4I_{13/2}\rightarrow{}^4I_{15/2}$	101.82	100	9.8	97.75	100	10.2	104.1	100	9.6	120.6	100	8.29
$^4I_{11/2}\rightarrow{}^4I_{15/2}$	83.20	80.4	9.7	77.9	79.9	10.3	86.0	80.7	9.4	105.6	81.8	7.74
$\rightarrow{}^4I_{13/2}$	20.30	19.6		19.6	20.1		20.6	19.3		23.57	18.2	
$^4I_{9/2}\rightarrow{}^4I_{15/2}$	69.54	69.1	9.9	63.48	68.3	10.7	67.9	67.8	9.9	106.92	73.9	6.92
$\rightarrow{}^4I_{13/2}$	29.15	29.0		27.51	29.6		30.3	30.2		35.65	24.7	
$\rightarrow{}^4I_{11/2}$	1.93	1.9		1.93	2.08		1.93	1.9		2.01	1.4	

serious. Meanwhile, the phenomenon of light-tight in AYF2 glass was much weaker compared with that of ZBLAN. The poor chemical stability against water attack of ZBLAN glass can degrade its otherwise outstanding optical properties.

Figure 3 indicates the absorption spectra of the samples at room temperature in the wavelength region of 300 nm–1900 nm. The shape and peak positions of each transition for the Er^{3+}-doped AlF_3-based glass are very similar to those in ZBLAN and other Er^{3+}-doped glasses[25,26]. The absorption bands corresponding to the transitions starting from the $^4I_{15/2}$ ground state to the higher levels $^4I_{13/2}$,$^4I_{11/2}$,$^4I_{9/2}$,$^4F_{9/2}$,$^4S_{3/2}$,$^2H_{11/2}$,$^4F_{7/2}$ were labeled. The absorption peak at 980 nm because of the $^4I_{15/2}\rightarrow{}^4I_{11/2}$ transition indicates the samples can be pumped by 980 nm laser efficiently.

Important spectroscopic and laser parameters of rare earth doped glasses have been commonly analyzed by many researchers using the Judd–Ofelt theory[27,28], hence, only the results will be presented. Table 3 shows the J-O parameters Ω_t of Er^{3+} in various glasses. Good agreement was found between the calculated and experimental values, the room mean-square error deviation of intensity parameters is $\times10^{-6}$, indicting the validity of the Judd-Ofelt theory for predicting the spectral intensities of Er^{3+} and the reliable calculations. Notably, that the ascending order of the parameters is $\Omega_2<\Omega_4<\Omega_6$ for the presented glasses, and the trend appeared similar to that of other rare earth doped fluoride glasses[27,29]. The Ω_2 is strongly dependent on the local environments of rare earth ion sites. The values of Ω_2 in fluoride glasses were smaller than those of heavy metal oxide glasses because the O^{2-} possesses higher covalency than F^-, and the fluoroaluminate glasses have lower covalency and higher asymmetry among the two main system of fluoride glasses.

Table 4 shows the calculated predicted spontaneous transition probability (A), radiaive lifetime (τ_{rad}), and branching ratio (β) of certain optical transitions for Er^{3+} - doped present glasses. The predicted spontaneous emission probabilities for Er^{3+}:$^4I_{11/2}\rightarrow{}^4I_{13/2}$ transition in fluoroaluminate glass was a little smaller than that of fluorozirconate glass owing to the lower refractive index, but owns higher branching ratio, which is beneficial to the 2.7 μm emission.

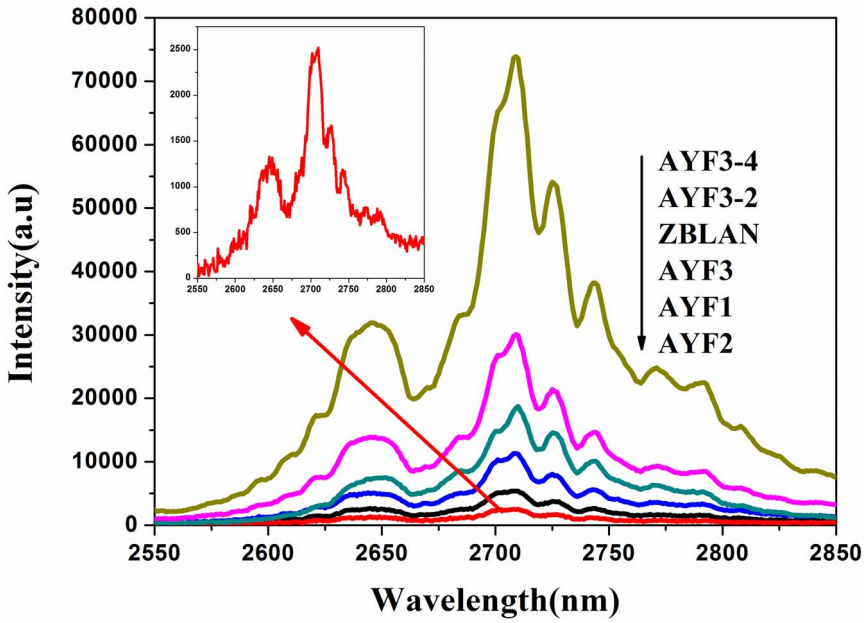

Figure 4 | The 2.7 emission spectra of present glasses under 980 nm diode laser excitation.

Under 980 nm diode laser excitation, the $^4I_{11/2}\rightarrow{}^4I_{13/2}$ fluorescence around 2.7 μm was obviously observed for the samples, as shown in Fig. 4. For Er^{3+}-doped fluoride glasses with different compositions, the emission peak occurs at similar wavelength. Although the AlF_3-based glasses possess lower intensity compared with the ZBLAN glass, their calculated emission cross sections at 2710 nm were 8.9, 9.4, and 8.8($\times10^{-21}$ cm^{-2}) similar to the value of ZBLAN (9.5×10^{-21} cm^{-2}). The lower intensity attributes to the OH^- absorption in AlF_3 –based glass. Enhanced 2.7 μm emission will be observed in our following work with the diminishment of the OH^- content and the adjustment of the composition. Moreover the intensity significantly increased when the concentration of Er^{3+} ions were added to the AYF_3-based-glass. It may be inferred that minimized concentration quenching occured in the 4 mol% Er^{3+}- doped fluoroaluminate glass. Higher concentration Er^{3+}-doped glasses can be studied further, and it is reasonable to believe these high chemically durable glasses may be considered to be a hopeful host for a 2.7 μm microchip laser and other optical laser application.

The emission cross section was calculated according to the Fuchtbauer-Ladenburg theory[30,31] and the absorption cross section (σ_{abs}) can be derived from the calculated σ_{em} using the McCumber equation[30]. On the basis of the σ_{abs} and σ_{em}, the wavelength dependence of the net gain[32] can be calculated as a function of population inversion for the upper laser level to determine qualitatively the gain property as follows:

$$G(\lambda) = P\times\sigma_e(\lambda) - (1-P)\times\sigma_a(\lambda) \quad (1)$$

where population inversion P is assigned to the concentration ratio of Er^{3+} in the $^4I_{11/2}$ and $^4I_{13/2}$ levels. As shown in Figure 5, the gain coefficients with various P values ranging from 0 to 1 were calculated for $^4I_{11/2}$—$^4I_{13/2}$ transition of the 1 mol% Er^{3+}-doped AYF2 glass (other AlF_3-based glasses and ZBLAN have similar spectra). Evidently, the positive gain was obtained when P>0.4, similar to the case in the ZBLAN glass[33] indicting that a low pumping threshold was achieved for the Er^{3+}:$^4I_{11/2}\rightarrow{}^4I_{13/2}$ laser operation.

AlF_3-based glasses (AlF_3-YF_3-CaF_2-BaF_2-SrF_2-MgF_2) with enhanced thermal and chemical stability were synthesized and compared with the well-known ZBLAN. All the prepared samples exhibited good glass-forming ability and did not show devitrification tendencies when being formed. Higher T_g (420+°C) of the AlF_3-based glasses compared with other various fluorozirconate glasses (270°C to 350°C) provides the glass good thermal stability to resist thermal damage at high pumping intensities. In addition, the characteristic temperatures of AlF_3-based glasses are larger than those of ZBLAN glass. The weight loss of ZBLAN in water was 30 times larger than that of AYF2 sample, and the concentration of cationic of ZBLAN in water was much larger than that of AYF2, which proves that the chemical stability of AYF2 was much better than that of ZBLAN glass. The emission properties and relevant parameters of the present samples were investigated and discussed. The fluoroaluminate glasses possessed large branching ratio (20%) along with emission cross section (9.4×10^{-21} cm^{-2}) of the Er^{3+}:$^4I_{11/2}\rightarrow{}^4I_{13/2}$ transition. Meanwhile, enhanced 2.7 μm emission in highly Er^{3+}-doped AYF glass was obtained. These results suggest that this kind of AlF_3-based fluoride glass has potential application in compact 2.7 μm lasers.

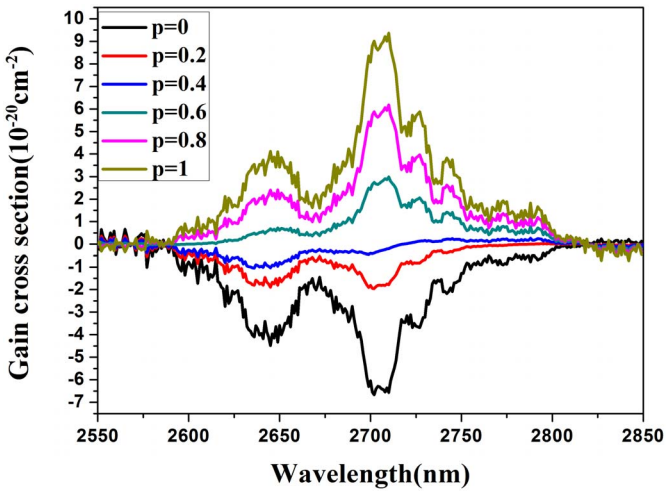

Figure 5 | Gain coefficients with the various P values ranging from 0 to 1 for $^4I_{11/2}$—$^4I_{13/2}$ transition of the 1 mol% Er^{3+}-doped AYF2 glass.

1. Yang, S. L., Wang, X. F. & Guo, H. T. Broadband near-infrared emission in Tm^{3+} - Dy^{3+} codoped amorphous chalcohalide films fabricated by pulsed laser deposition. *Opt. Express.* **19**, 26529–26535 (2011).
2. Jackson, S. D., King, T. A. & Pollnau, M. Diode Pumped Erbium Cascade Fiber Laser. *Opt. Lett.* **24**, 1133–1135 (1999).
3. Tsang, Y. H., El-Taher, A. E. & King, T. A. Efficient 2.96 μm dysprosium-doped fluoride fibre laser pumped with a Nd:YAG laser operating at 1.3 μm. *Opt. Express.* **14**, 678–685 (2006).
4. Jackon, S. D. *et al.* Diode-pumped fiber lasers: A new clinical ccol? *Laser in Surgery and Medicine* **30**, 184–190 (2002).
5. Wesendahl, T. *et al.* Erbium:YAG Laser Ablation of Retinal Tissue under Perfluorodecaline: Determination of Laser–Tissue Interaction in Pig Eyes. *Invest Ophthalmol Vis Sci* **41**, 505–512 (2000).
6. Zhu, X. & Jain, R. Compact 2 W wavelength-tunable ErZBLAN. *Opt. Lett* **32**, 2381–2383 (2007).
7. Iqbal, T. *et al.* Synthesis, Characterization, and potential application of highly chemically durable glasses based on AlF_3. *Meaterials Reacher Society* **6**, 410–406 (1991).
8. Zhu, X. & Jain, R. 10-W-level diode-pumped compact 2.78 μm ZBLAN fiber laser. *Opt. Lett* **32**, 26–28 (2007).
9. Faucher, D., Bernier, M. & Androz, G. 20Wpassively cooled single-mode all-fiber laser at 28 μm. *Opt. Lett* **36**, 7–9 (2011).
10. Tokita, S., Hirokane, M. Y., Murakami, M., Shimizu, S. & Hashida, M. Stable 10 Er:ZBLAN fiber laser operating at 2.71–2.88 μm. *Opt. Lett* **35**, 3943–3946 (2010).
11. Zhu, X. & Peyghambarian, N. High-Power ZBLAN Glass Fiber Lasers: Review and Prospect. *Advances in OptoElectronics* **2010**, 1–23 (2010).
12. Richards, B. D. O. *et al.* Mid-IR (3–4 μm) fluorescence and ASE studies in Dy^{3+}doped tellurite and germanate glasses and a fs laser inscribed waveguide. *Laser Phys Lett* **10**, 085802 (2013).
13. Rhonehouse, D. L. *et al.* Low loss, wide transparency, robust tellurite glass fibers for mid-IR (2 – 5 μm) applications. *SPIE* **8898**, 88980D (2013).
14. Guo, Y. Y. & Li, M. Intense 2.7 μm emission and structuralorigin in Er^{3+}-doped bismuthate (Bi_2O_3-GeO_2-Ga_2O_3-Na_2O) glass. *Opt. Lett* **37**, 268–270 (2012).
15. Xu, R. & Tian, Y. Enhanced emission of 2.7 μm pumped by laser diode from Er^{3+}/Pr3+codoped germanate glasses. *Opt. Lett* **36**, 1173–1176 (2011).
16. Frischat, G. H., Hueber, B. & Ramdohr, B. Chemical stability of ZrF_4- and AlF_3-based heavy metal fluorode glass in water. *J Non-Cryst. soilds* **284**, 105–109 (2001).
17. Yanagita, H., Toratani, H., Yamashita, T. T. & Masuda, I. Diode pumped E^{r3+} glass laser at 2.7 μm. *SPIE* **1513**, 386–395 (1991).
18. Santos, F. A. *et al.* Thermal stability and crystallization behavior of TiO_2 doped ZBLAN glasses. *J Non-Cryst. soilds.* **357**, 2907–2910 (2011).
19. Tian, Y. *et al.* 1.8 μm emission of highy thulium doped fluorophosphate glasses. *J Appl. Phys* **108**, 083504 (2010).
20. Xu, R. *et al.* 2.05 μm emission properties and energy transfer mechanism of germanate glass doped with Ho^{3+}, Tm^{3+}, and Er^{3+}. *J Appl. Phys.* **109**, 053503 (2011).
21. Al-Allak, H. M. *et al.* The effect of Mn on the positive temperature coefficient of resistance characteristics of donor doped $BaTiO_3$ ceramics. *J Appl. Phys* **63**, 4530 (1988).
22. Lebullenger, R. *et al.* Systematic substitutions in ZBLA and ZBLAN glasses. *J Non-Cryst. soilds* **161**, 1217–221 (1993).
23. Tian, Y. *et al.* 2.7 μm fluorescence radiative dynamics and energy transfer between Er^{3+} and Tm^{3+} ions in fluoride glass under 800 nm and 980 nm excitation. *Journal of Quantitative Spectroscopy and Radiative Transfer* **113**, 87–95 (2012).
24. Guo, Y. *et al.* Er^{3+}-doped fluoro-tellurite glass: A new choice for 2.7 μm lasers. *Mater Lett.* **80**, 56–58 (2012).
25. Shinn, M. D. *et al.* Optical transitions of Er^{3+} ions in fluorozirconate glass. *Phys. Rev.* **27**, 6635–6648 (1983).
26. Chen, Y., Wen, L. & Hu, L. Raman and optical absorption spectroscopic investigation of Yb-Er codoped phosphate glasses containing SiO_2. *Opt. Lett* **7**, 56–59 (2009).
27. Ivanova, S. & Pelle, F. Strong 1.53 to NIR–VIS–UV upconversion in Er-doped fluoride glass for high-efficiency solar cells. *J. Opt. Soc. Am. B.* **26**, 1930–1939 (2009).
28. Lin, H., Chen, D. & Yu, Y. Enhance mid-infrared emissions of Er^{3+} at 2.7 μm via Nd^{3+} sensitization in chalcohalide glass. *Opt. Lett.* **36**, 1815–1817 (2011).

29. Tian, Y. *et al*. Spectroscopic properties and energy transfer process in Er^{3+} doped ZrF_4-based fluoride glass for 2.7 μm laser materials. *Opt. Mater.* **34**, 308–312 (2011).
30. Zou, X. & Izumitani, T. Spectroscopic properties and mechanisms of excited state absorption and energy transfer upconversion for Er^{3+}-doped glasses. *J Non-Cryst. soilds.* **162**, 68–80 (1993).
31. Schweizer, T. *et al*. Spectroscopic data of the 1.8-, 2.9-, and 4.3-mm transitions in dysprosium-doped gallium lanthanum sulfide glass. *Opt. Lett.* **21**, 1594–1596 (1996).
32. Miniscalco, W. J. & Quimby, R. S. General procedure for the analysis of Er^{3+} cross section. *Opt. Lett.* **16**, 258–260 (1991).
33. Zou, X. & Toratani, H. Spectroscopic properties and energy transfers in Tm^{3+} singly- and Tm^{3+}/Ho^{3+} doubly- doped glasses. *J Non-Cryst. soilds.* **195**, 113–124 (1996).
34. Wang, B. *et al*. Infrared excited-stated absorption and stimulted-emission cross section of Er $^{3+}$-doped c rystals. *Opt. Mater* **31**, 1658 (2009).

Acknowledgments

This work is financially supported by National Natural Science Foundation of China (No. 51172252).

Author contributions

F.H. wrote the main manuscript text and coauthor Y.M., W.L. and X.L. checked up. D.C. and L.H. are responsible for the experiment. All authors reviewed the manuscript.

Additional information

Competing financial interests: The authors declare no competing financial interests.

How to cite this article: Huang, F.F. *et al*. 2.7 μm emission of high thermally and chemically durable glasses based on AlF_3. *Sci. Rep.* **4**, 3607; DOI:10.1038/srep03607 (2014).